FERMILAB-PUB-23-793-STUDENT

Mu2e - Research & Development

by

Alexis Bibian

Science Undergraduate Laboratory Internships (SULI), Department of Energy at Fermi National Laboratory, 2023

In partial fulfillment of the requirements

for the completion of

SULI Deliverable Requirements

Nov, 2023

ABSTRACT

Current efforts are being conducted at Fermi National Laboratory to study potential violations in accepted theory that would otherwise suggest a restructuring of our fundamental understanding of the universe. Mu2e is one of these frontier projects that studies Charged Lepton Flavor Violation (CLFV) which if observed, would suggest physics beyond the Standard Model. Therefore, this note encompasses several projects that contribute to the fruition of Mu2e investigations. Due to the broad range of disciplinary inconsistencies that each project requires, all the work is being presented as a means of justifying contribution to Mu2e. The projects are comprised of a simulation exploring the extinction level of proton pulses after Recycler ring re-bunching by using G4beamline to simulate an 8GeV proton beam interaction with a titanium target, three Cherenkov radiation-based detectors and 2/3-fold and 3/3-fold coincidence rate analysis. Additionally, supplemental work for the implementation of a Micro Telecommunications Computing Architecture (TCA) crate to establish a peak finding algorithm to ensure that the out-of-time beam is less than 10^{-10} fractional level along with single-layer inefficiency analysis on scintillation counters for the Cosmic-Ray Veto (CRV) analysis to ensure the overall inefficiency is 10^{-4}. Preliminary results have been achieved for the G4beamline simulation 2/3-fold and 3/3-fold coincidences which are in the order of 10^{-9} and 10^{-10}, respectively. Only preliminary results of a triangular counter and four rectangular di-counters for the CRV have been realized. The microTCA crate development is still ongoing.

Contents

List of Figures

Abbreviations

CLFV Charged Lepton Flavor Violation. i

CRV Cosmic-Ray Veto. i

FPGA Field Programmable Gate Array. 17

PE Photo-Electron. 8

SiPMs Silicon Photo-Multipliers. 7

TCA Telecommunications Computing Architecture. i

UEM Upstream Extinction Monitor. 5

Chapter 1

INTRODUCTION - MU2E EXPERIMENT

1.1 Objective & Interactions

The objective of Mu2e is to explore the violation of the conservation laws that's described by the Standard Model. In this case, charged lepton flavor violations (CLFV) are being explored through the muon-to-electron transitions [1]. When analyzing transitions in these scales, the outcome can only be probabilistic in nature meaning that there can only be a few probable outcomes. The interaction being analyzed in this case is a muon particle being captured by an aluminum atom [2]. This interaction will produce one of three outcomes. The most probable outcome will be the decay of the muon-to-electron and two neutrinos after the muon replaces an electron on the aluminum atom.

$$\mu^- \rightarrow e^- + \bar{\nu}_e + \nu_\mu \tag{1.1}$$

Another possible outcome is nuclear capture by the aluminum atom. This process will cause the muon to change one of the protons to a neutron and in the process, produce a neutrino.

$$p + \mu^- \rightarrow n + \nu_\mu \tag{1.2}$$

The last outcome is a prediction that has not yet been observed and gives its purpose to Mu2e, direct conversion of a muon-to-electron without the production of neutrinos. This is considered a violation of one of the fundamental laws that gives the Standard Model such an effective outcome, which is conservation of lepton number.

$$\mu^- \rightarrow e^- \tag{1.3}$$

As seen in Eq. 1.3, there is $L_\mu = 1$ and $L_e = 0$ on the left-hand side and $L_\mu = 0$ and $L_e = 1$ on the right-hand side which creates a miss match in lepton number, thus, CLFV is observed. This neutrino-less conversion will produce an electron with energy slightly less than the rest mass of the muon through the additional influence of the aluminum nucleus. This will produce an electron with an energy of 104.97MeV. The Mu2e experiment setup

is seen in Figures 1.1 and 1.2.

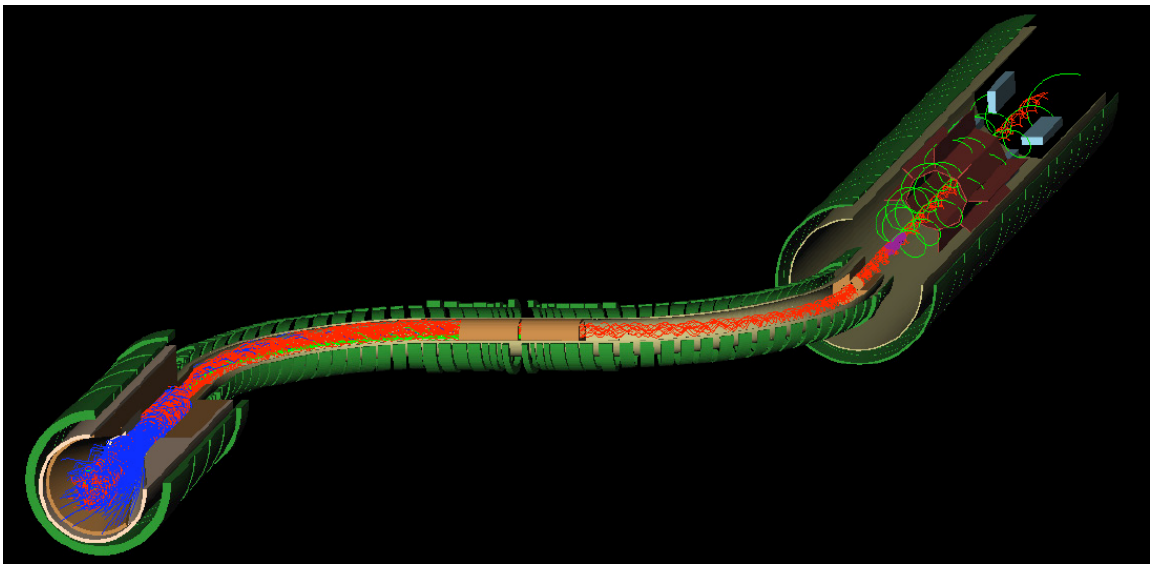

Figure 1.1: A G4beamline simulation displaying the Mu2e experiment setup showing the protons (blue tracks) with a forward scattering after interaction with the target and the negatively charged pions and muons (red particles) with some neutral particles (green) heading back, towards the detector [3].

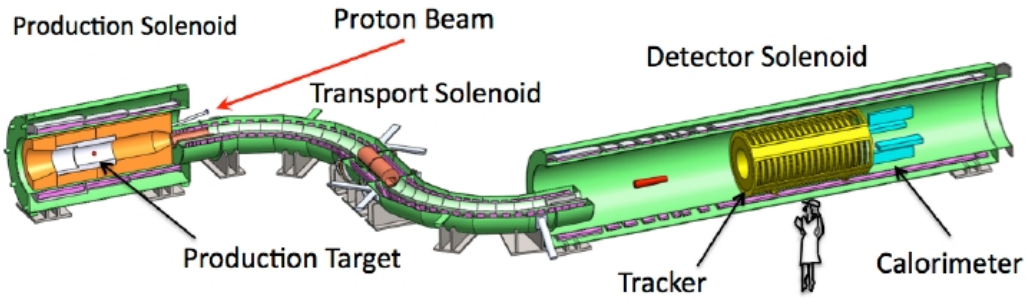

Figure 1.2: This image displays the three solenoids along with the path trajectory of the muon beam.

1.2 Recycler Ring & Backgrounds

As stated previously, the sensitivity of Mu2e is very restrictive on the timing profiles of each pulse meaning that the out-of-time beam needs to be within a certain magnitude to be able to accurately detect CLFV. Therefore, this section encompasses the largest contributing sources to bad sensitivity. Below is a list of five sources of biggest concern:

1. Scale of beam intensity driven processes that can induce muon decay in orbit and muon capture by nucleus.

2. Interactions produced by delayed particles other than muons incident on the stopping target.

3. Interactions that produce electrons with a near coincidence in time with the arrival of the particle at the stopping target.

4. Interactions induced by cosmic rays, producing electrons or muons mimicking beam interactions.

5. Conventional processes producing events by activity in the detector.

The temporal requirements of the incident proton beam of Mu2e can be summed up in the extinction requirement which requires that no beam be present between pulses at the 10^{-10} fractional level assuming that the out-of-time particles are uniformly distributed. The extinction requirement will minimize the probability of out-of-time beam interactions with the muon stopping target to ensure that minimal-to-no activity in between pulses is detected.

1.2.1 Re-Bunching:

Prior to the muon beam production, the proton beam pulses need to be restructured both spatially and temporally. This restructuring of the proton pulses is known as re-bunching. In this process, the bunches are restructured from 53 MHz pulses from the Booster to 2.5 MHz pulses in the Recycler ring [4]. This allows for the new 2.5 MHz pulses to achieve the proper time profiles that Mu2e requires.

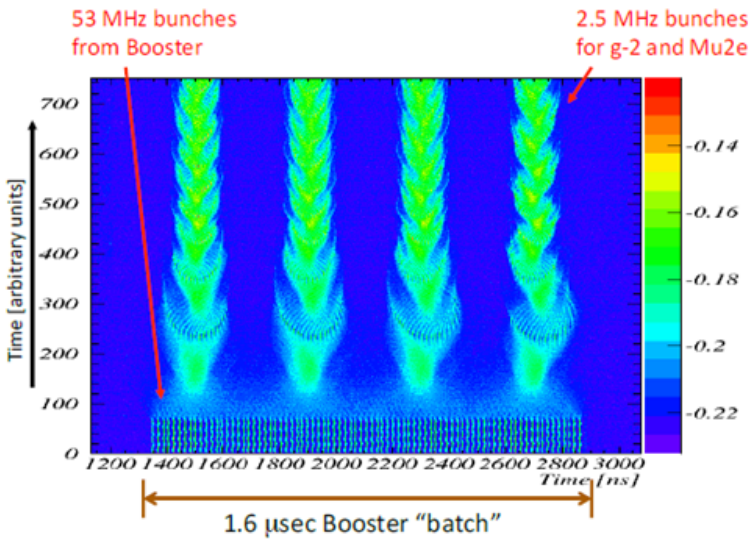

Figure 1.3: Waterfall plot of the re-bunching formation starting with 8 GeV at a frequency of 53 MHz from the Booster ring to 2.5 MHz in the Recycler ring with a total time of 90 ms bunch formation [4].

The Recycler ring forms 4 bunches from 1.6 μsec batch from the Booster ring then a single bunch is transferred to the Delivery ring to initiate injection. This is possible due to a high speed "kicker" which will transfer the reshaped bunches one-by-one to the Delivery ring. Preliminary simulations have been conducted that suggest 10^{-5} extinction levels are achievable in the Recycler ring. From this bunch formation process, the following time profile seen in Figure 1.4 can ultimately be formed to satisfy the extinction requirement to be no worse than 10^{-10} level [5].

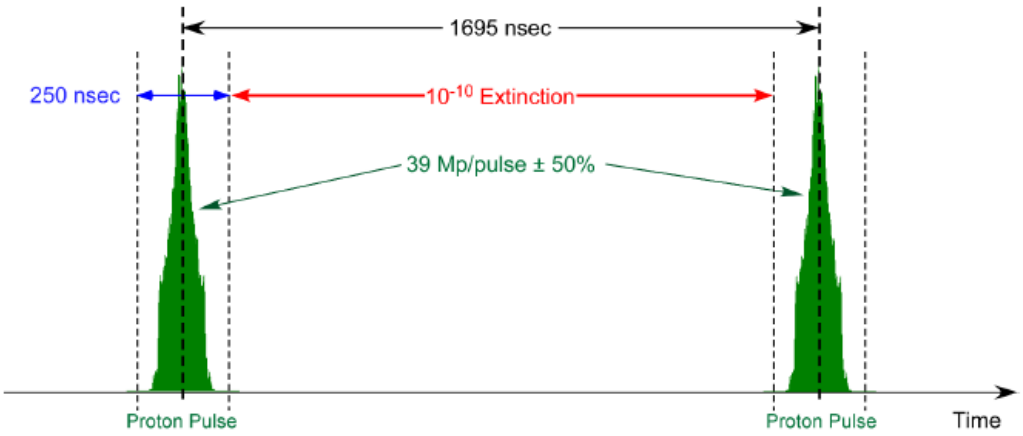

Figure 1.4: This is the pulsating time profile of the proton beam that will allow for the extinction requirement for Mu2e to be met [5].

1.2.2 Extinction:

Beam extinction is the ratio of out-of-time (in between pulses) particles striking the target to the total number of particles in-time (during beam pulse) striking the target. This requirement predicts the rate of interactions that could falsify signals due to particles arriving late, thus, hinting to CLFV. Therefore, different measures are being implemented at different locations in the beamline to reduce such signals of no concern. The high-speed "kicker" is an example of one technique that's used for that purpose. To ensure that the extinction requirement is met, AC dipoles and collimators are situated downstream of the Delivery ring, prior to the Production Solenoid, so that only the in-time proton pulses are transported to the Production Solenoid further enhancing the extinction levels to about 10^{-7}. Additionally, the pulsed beam allows for a statistical approach to be implemented using a detector with a fast time resolution along with a small effective acceptance rate to build a time profile over many bunches. All of this, plus considerations on other background sources such as cosmic rays or antiprotons will all be used to meet the extinction requirement of 10^{-10}. The different locations of each of the extinction procedures are seen in Figure 1.5 and can be referenced to [6].

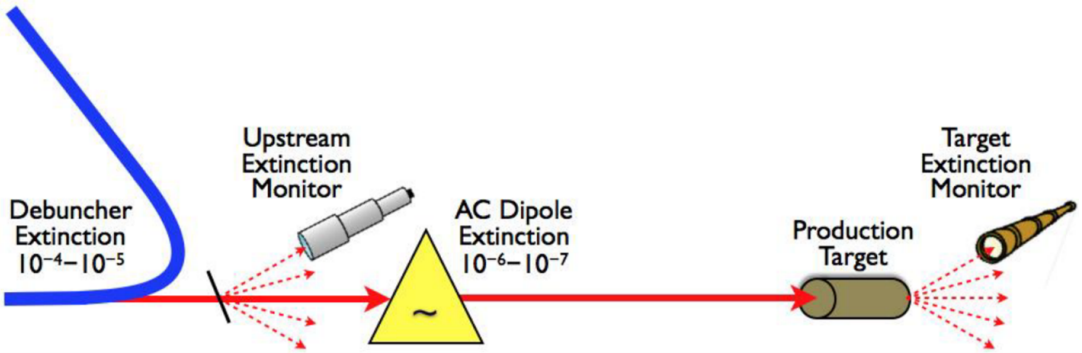

Figure 1.5: The out-of-time extinction of the proton beam after ejection from the Delivery ring all the way up to the Production Target interaction in the Production Solenoid [6].

Upstream Extinction Monitor:

The Upstream Extinction Monitor (UEM) has the purpose of analyzing the temporal width and intensity of the proton pulses downstream of the AC dipole and collimators. This can be used to check for any discrepancies or malfunctions in the accelerator complex which will allow for a quick diagnosis and isolation of such potential issues. The location of the UEM is seen in Figures 1.6 and 1.7 and was chosen also for the purpose of beam commissioning to be able to tune the upstream accelerator complex.

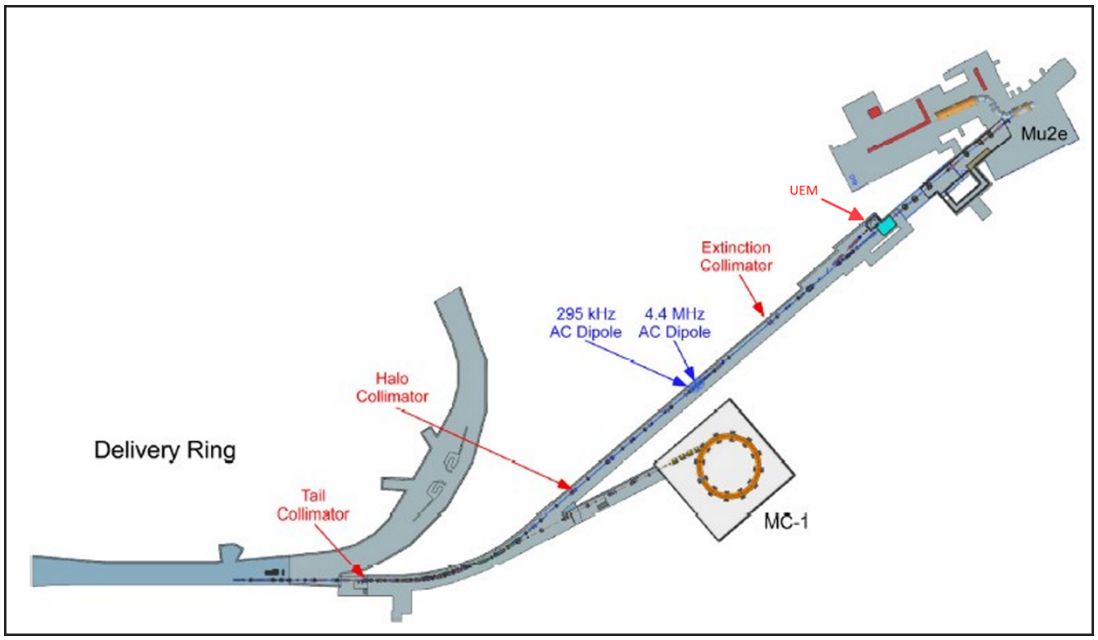

Figure 1.6: A map of the beam path after the Delivery ring, showing the different beam pipes that lead to muon campus.

The telescope detector will use 2/3- and 3/3-fold coincidences of the scattered particles to determine the rate of scattered particles per incident proton. This can be used to estimate the amount of particles expected at the UEM telescope using the estimated extinction level in that region. The simulation using G4beamline will allow for prelimenary estimates of the rate of scattered particles using both coincidence rates to display looser and tighter

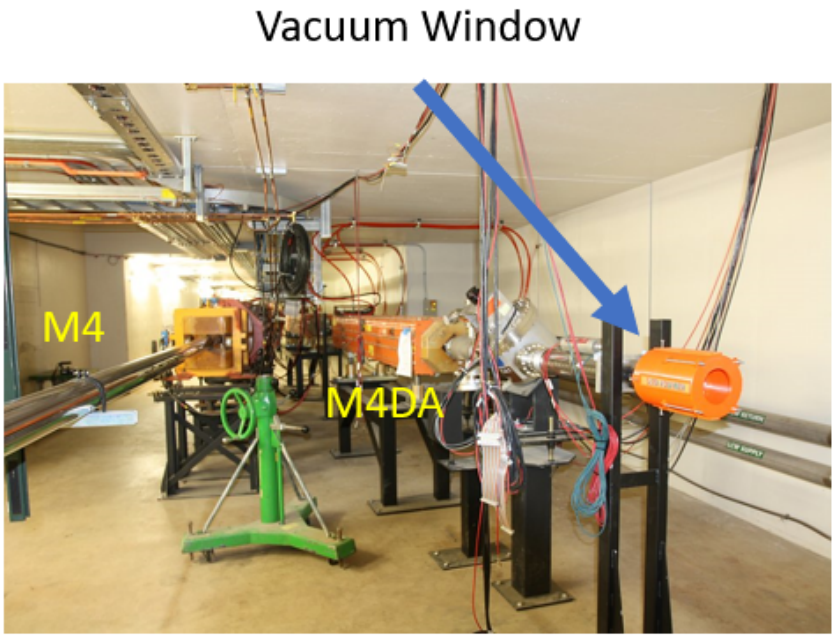

Figure 1.7: A closer look at the beamline where the UEM setup will be installed to analyze extinction.

requirements to showcase acceptable sensitivity. The rates can then be used to determine the number of expected particles between proton pulses over many pulses. The physical setup that the simulation will replicate is seen in Figure 1.8.

Figure 1.8: The real setup showing the target position with respect to the angled telescope detector setup.

G4beamline:

G4beamline is a simulation program optimized for accurate and realistic implementation of beamline setups through single-particle simulation. It's based on Geant4 toolkit and has the capabilities to simulate particle transports in matter and electromagnetic fields. Additionally, it was used to simulate the particle tracking in the Mu2e setup after muon beam production as discussed [3]. Further clarification of commands and other simulation program usage can be found in the G4beamline User's Manual [7].

1.2.3 Cosmic Ray Veto:

The CRV investigations strive to also minimize interactions that would otherwise suggest stopping target processes hinting at CLFV [8] through the production of 105MeV electrons as seen in Figure 1.9. These interactions can be caused by cosmic-ray muons in the target, or the muons can mimic the electrons themselves causing a signal [9]. Due to this, four long extruded layers of scintillation panels with aluminum absorbers between the layers will be implemented to cover the Detector Solenoid to ensure that all cosmic-ray muons are vetoed in the offline analysis of each run. The CRV enclosure is seen below in Figure 1.10.

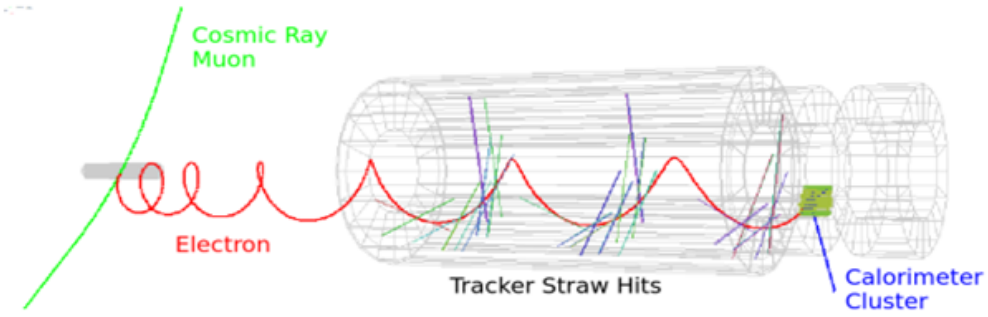

Figure 1.9: This image displays one of the concerning interactions from a cosmic-ray muon interacting with the stopping target, producing an electron in the Detector Solenoid [9].

CRV Modules:

The analysis is conducted using Silicon Photo-Multipliers (SiPMs) cells to construct a series of channels that run along the length of the extruded panels. Embedded wavelength-shifting fibers capture the light from the photoelectron excitation of the counters and are detected at the end of each extruded panel. The long-extruded scintillation modules are studied and tested to ensure that they meet the overall efficiency requirement of 99.99%. This constitutes an overall inefficiency of 10^{-4} [10]. The modules and setup can be seen in Figures 1.11 and 1.12. There is a total of 4 CRV modules with 4 panel layers each stacked on top of each other implying that there are a total of 16 layers of di-counters. From this setup, studies can then be made to ensure that the modules can account for muonic activity

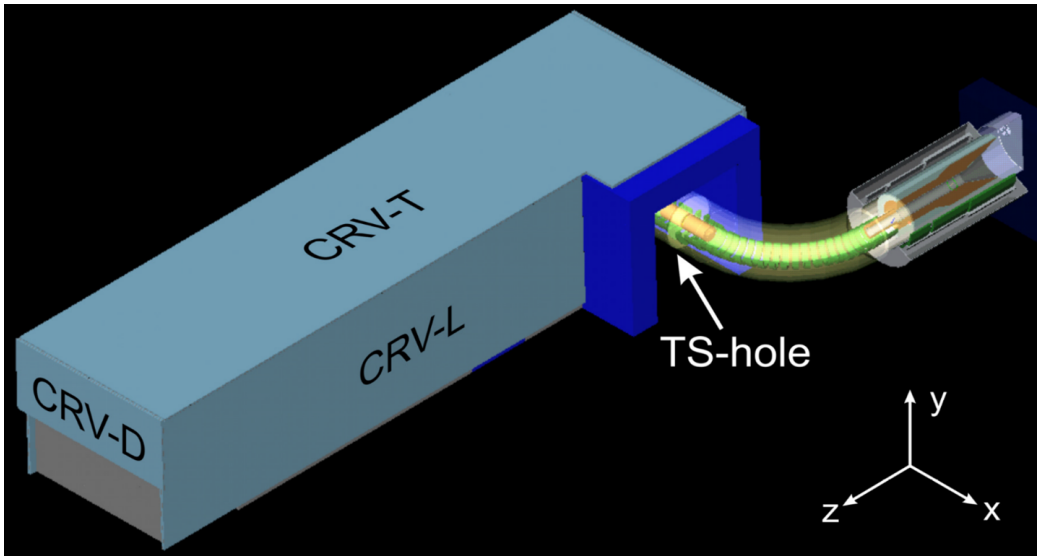

Figure 1.10: The CRV enclosure setup when implemented in the final Mu2e experiment.

from cosmic rays by analyzing the tracks that these events create. A coincidence-based approach will be conducted to trace the muon tracks by filtering showers and all other cosmic radiation that doesn't fall within the cosmic ray track requirements. This will then be used to ensure that all cosmic muons are accounted for when analyzing interactions that can mimic muon signals or induce interactions in the stopping target. Thus, the overall efficiency across all modules on all sides (CRV-D, CRV-T, CRV-L, etc.) must be 99.99% or overall inefficiency of 10^{-4}.

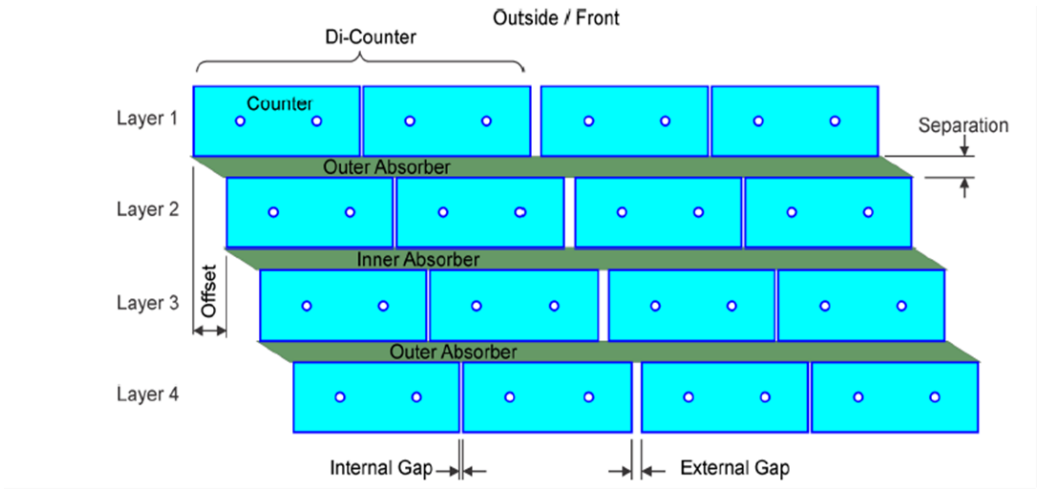

Figure 1.11: A section of a module depicting the di-counters with all four layers [10].

A cosmic-ray muon is a coincidence hit, if it hits in three locally adjacent counters in the four layers. To ensure that the inefficiency requirement of 1×10^{-4} is met, a single-layer inefficiency analysis will be conducted using counter Photo-Electron (PE) yield requirement. To meet the overall inefficiency requirement, a single-layer inefficiency of 0.4% for a four-layer cosmic ray veto is needed.

Figure 1.12: The physical depiction of the modules stacked on top of each other along with the storage unit they're kept in at Fermilab.

Chapter 2

UPSTREAM EXTINCTION MONITOR ANALYSIS

2.1 Objective

The purpose of this project is to simulate the scattering interaction of the 8GeV proton beam with a thin titanium target using G4beamline, a geant4-based program, to obtain preliminary predictions of the scattered particles per proton using 2/3- and 3/3-fold coincidences. This will provide information of the out-of-time beam based on the expected extinction level expected in that location and the in-time beam to ultimately make the physical measurement and ensure that the extinction is 10^{-10} level over many pulses in the Production Solenoid.

2.2 Background

This Upstream Extinction Monitor uses a telescope system with quartz crystals to ensure that the response time is fast enough so that no residual signals from the in-time pulse overlap with the consecutive out-of-time signal or the subsequent proton pulse. This process is referred to as the dead time of the detector. The detector will analyze the charged scattering production of the proton pulses with the titanium target as seen in Figure 2.1. Along with the fast response of a quartz crystal PMT detector, the periodic structure of the pulses will allow for a statistical approach to attain a precise distribution over many pulses. The pulses will interact with the titanium target which will allow for most of the 8GeV beam to pass through, only scattering a small fraction. This small fraction will be analyzed by the telescope system using Cherenkov radiation.

Cherenkov radiation is the production of photons due to charged particles traveling faster than the speed of light in a transparent medium. This is observed in nuclear reactors through the produced charged particles' interaction with water. In this case, the medium is a quartz crystal with a refractive index of 1.47. The velocity of the particle traversing through the crystals is the defining condition to produce Cherenkov radiation. This condition is seen in Eq. 2.1.

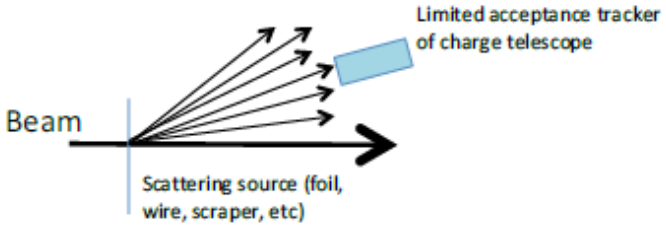

Figure 2.1: A schematic of the telescope system with respect to the incident beam.

$$\beta > \frac{1}{n} \tag{2.1}$$

Where $\beta = v/c$, n is the index of refraction of the material, v is the velocity of the particle, and c refers to the speed of light which can all be translated to define the threshold velocity with

$$v_{th} > \frac{c}{n} \tag{2.2}$$

Using the 1.47 index of refraction of the quartz crystals, $\beta > 0.680$ or $v > 203,401,360$ m/s. This condition can then be used to determine the individual particle's threshold kinetic energies which can be determined using Eq. 2.3.

$$T_{th} = [(1 - \frac{v_{th}^2}{c^2})^{-1/2} - 1]m_0c^2 \tag{2.3}$$

Where m_0 is the rest mass of the particle in question. G4beamline outputs the data in a text file with the individual momentum components therefore, Eq. 2.3 must be translated to a momentum threshold equation as described by Eq. 2.4.

$$P_{th} = \sqrt{(E_0 + T_{th})^2 - E_0^2} \tag{2.4}$$

Where E_0 is the rest or potential energy of the particle. Using these conditions and relations, the following chart can be built of the charged particles produced in this interaction.

Particle Parameters					
	m_0 (MeV/c^2)	E_0 (MeV)	T (MeV)	P_{th}(MeV/c)	PDGid
e	0.511	0.511	0.185	0.473	11
μ	105.700	105.700	38.266	97.742	13
π	140.000	140.000	50.683	129.460	211
p	938.272	938.272	339.673	867.635	2212

Figure 2.2: A list of the charged particles with their associated identifiable properties. PDGID is the identification value that G4beamline assigns to the particles based on the Particle Data Group.

2.3 Equipment & Procedure

The exact setup contains three quartz crystals and three PMTs. The quartz crystals being used in the physical experiment are seen in Figure 2.3 and the PMT assembly is seen in Figure 2.4. This process is done to all three PMT assemblies then mounted in line with one another on an arm as seen in Figure 2.5. It follows the schematic seen in Figure 2.6 with respective dimensions.

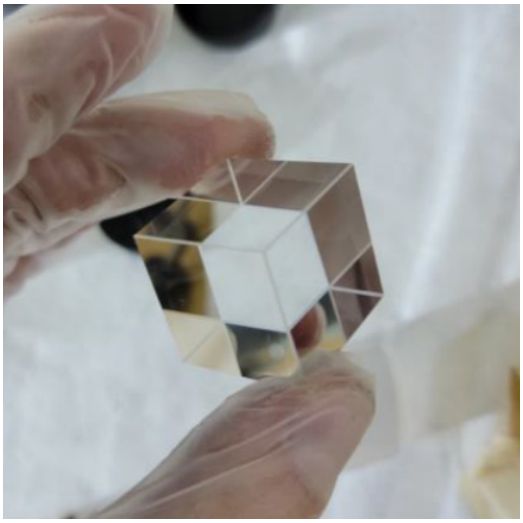

Figure 2.3: One of the quartz crystals that'll be used as the signal source for the PMT.

Figure 2.4: The PMT assembly depicting the cylindrical housing at the top, PMT with end-cap in the bottom left, and quartz crystal in the holder on the bottom right.

Taking all of this to create the most accurate setup in G4beamline using the dimensions of the physical components gives us the setup seen in Figure 2.7. The three PMT detectors will use coincidences as the foundation for the statistical analysis. More specifically, 2/3-fold and 3/3-fold coincidences will be analyzed to produce two separate coincidence rates, respectively. This will allow for a closer look at how the more stringent requirement, 3/3-fold requirement is affected in comparison to the more accepting 2/3-fold requirement. Based on this coincidence analysis, particles will be tracked through track IDs produced by G4beamline to identify the particles that meet all requirements traversing through two or all three crystals. This will account for particles that decay into other charged particles halfway through traversing the telescope. For example, if a photon excites and generates an electron in the first crystal that goes on to interact with the two remaining crystals with

Figure 2.5: The three PMTs are installed on the arm prior to installation.

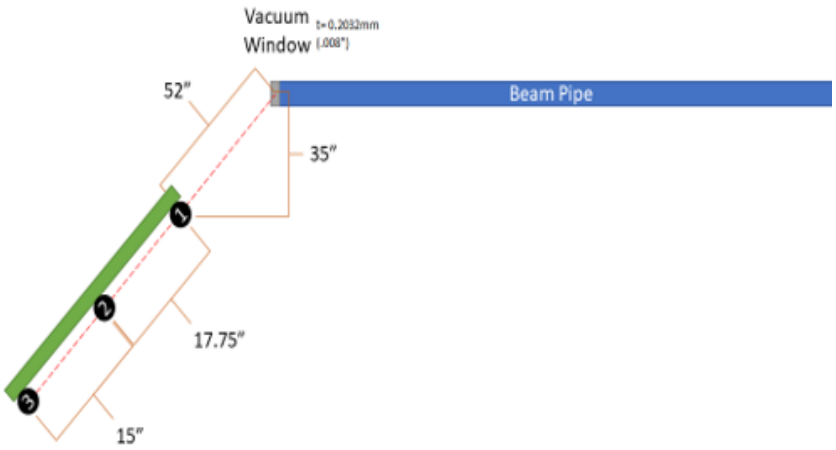

Figure 2.6: A schematic of the setup, similar to Figure 2.1, with the depicting the dimensions.

sufficient velocity to generate Cherenkov radiation, it'll be considered a 2/3-fold coincidence, not accounting for the photon. The simulation will run in a supercomputer for ten trials with a proton count of 10^9 incident on the titanium target.

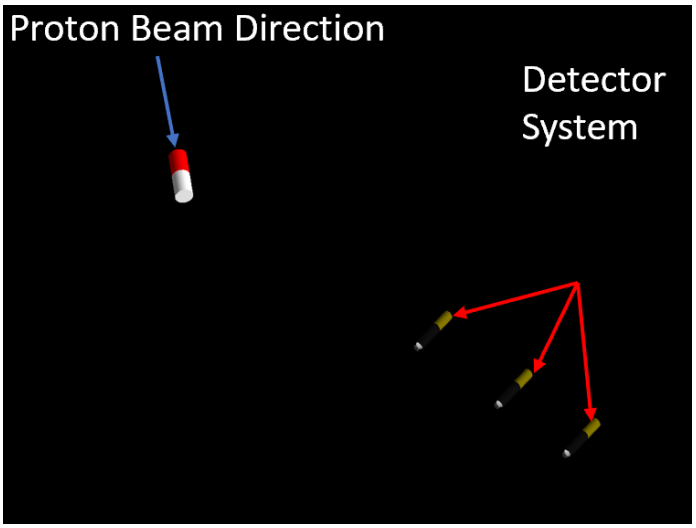

(a)

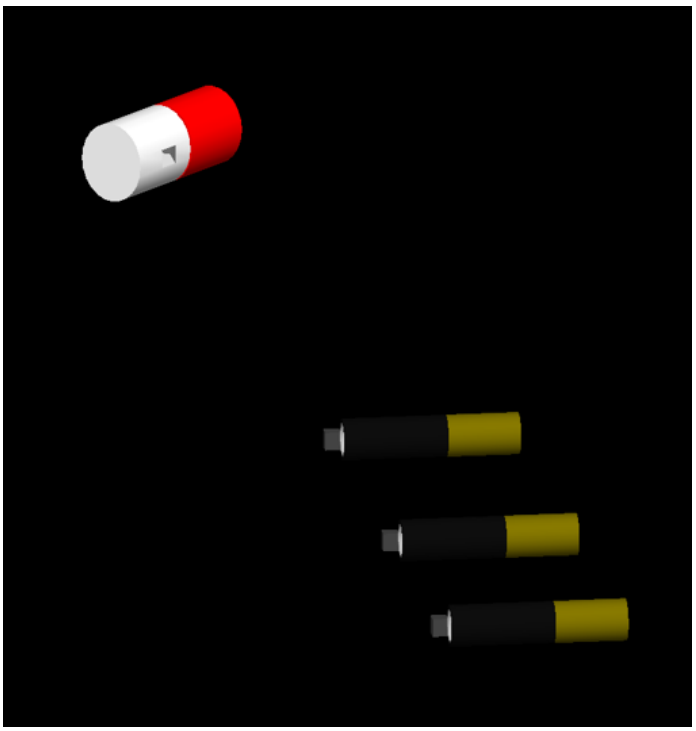

(b)

Figure 2.7: The simulated G4beamline setup used for the extinction rate analysis. The titanium target is in between the white and red cylinders.

2.4 Results

Each crystal produced an associated txt file with the list of particles that traverse through it with the associated particle properties such as momentum P_x, P_y, and P_z separately, particle ID (PDGid), and track ID. These txt files are produced by the BLTrackFile command in the input code seen in Appendix A. Therefore, the data processing of the raw txt files is conducted in Excel using the Power Query features which is an Excel extension used for importing and connecting external data files for live data processing. This allowed for the incorporation of data filters to only extract the charged particles that produce Cherenkov radiation. There are a total of four filters:

1. Only charged particles are registered.
2. Outputs charged particles that only interact with two or all three crystals.
3. Eliminates photons.
4. Outputs particles that meet their momentum threshold, respectively.

The first filter is done in G4beamline, all other filters were done in Excel. The second filter drastically decreases the number of particles since the probability that the particle will pass through two or let alone, all three crystals is low. The proton pulse also has a low probability of scattering from the thin titanium target, producing a small number of scattered particles detected by the telescope. In most trials, no particles survived but the

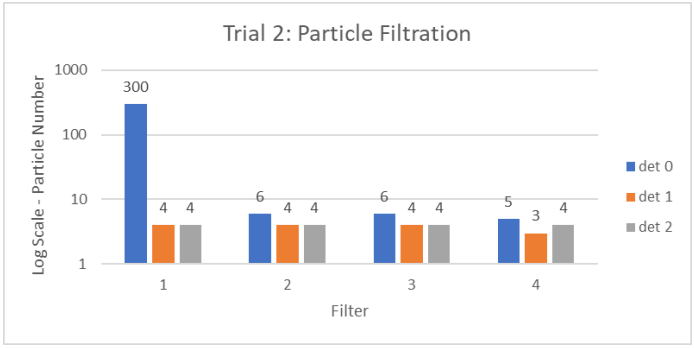

(a)

Filter	N particles		
	det 0	det 1	det 2
1	300	4	4
2	6	4	4
3	6	4	4
4	5	3	4

(b)

Figure 2.8: A depiction of the rapid decrease in the number of particles as a function of the filter from trial 2.

results still aid by providing statistical relevance. After averaging the number of particles that passed the filtration system across all trials, the average was 5 particles.

The coincidence rates are then calculated by normalizing the particles that passed all the filters with the total number of particles in the proton pulse. From this, all the coincidence rates for all trials can be determined and averaged to get a statistical interpretation of the 2/3-fold and 3/3-fold coincidence rates which is shown in the chart in Figure 2.9. The 2/3-fold rate averaged out to be $(2.2 \pm 1.5) \times 10^{-9}$ and the 3/3-fold rate is $(3.0 \pm 2.1) \times 10^{-10}$.

Coincidence Rates		
Trials	2/3-fold Rate	3/3-fold Rate
1	0	0
2	1.0E-09	1.0E-09
3	5.0E-09	2.0E-09
4	0	0
5	0	0
6	0	0
7	0	0
8	0	0
9	1.0E-09	0
10	1.5E-08	0
Average	2.2E-09	3.0E-10
STDEV Mean	1.5E-09	2.1E-10

Figure 2.9: Coincidence rates for all the ten trials with the associated average and standard deviation.

2.5 Conclusion

The simulated extinction rate interaction using a titanium target with the 8GeV proton beam produces a 2/3-fold coincidence rate of $(2.2 \pm 1.5) \times 10^{-9}$ and a 3/3-fold coincidence rate of $(3.0 \pm 2.1) \times 10^{-10}$. This is consistent with the expected rates based on the statistical approach. This confirmation will aid in the verification of out-of-time beam prior to the Production target to ensure the 10^{-10} extinction requirement is met.

Chapter 3

SUPPLEMENTAL WORK

3.1 Projects

Supplemental work refers to work that was conducted but doesn't contain sufficient development to be a stand-alone project like the one discussed previously. In this case, there are only two projects that fit this criterion which is the development of a UEM microTCA crate to implement a peak finding algorithm using a Field Programmable Gate Array (FPGA). The other project is the CRV development which analyzes the counters' inefficiency of detecting cosmic muon signals.

3.2 microTCA Crate

The crate is intended to be used to test the coincidence rates of the statistical analysis using G4beamline simulation just discussed in the previous chapter. The purpose of this is to verify whether the rates are about the same factor or not. This will provide insight into potential malfunctions in the physical tests or in the G4beamline code. Figures 3.1 and 3.2 show depictions of the algorithm that'll be used to process the PMT signals and the overall schematic of the crate.

To get this algorithm working, a Linux machine must be set up with Vivado 2016.2. From there, the code can be completed using VHDL coding language then the crate assembled. The work that was conducted for this project was the setup of the Linux machine where the code will be built and ensuring all the components for the crate are accounted for with minor assembly of the crate. Due to time constraints, no other work was conducted for the development of the microTCA project.

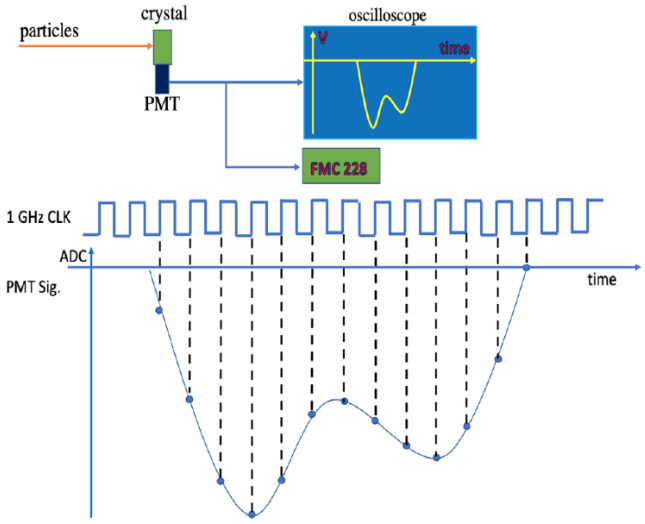

Figure 3.1: A schematic depicting the setup of the microTCA and how the signal from the crystals will propagate to the crate along with mapping of the analog signal to ADC using a 1 GHz clock.

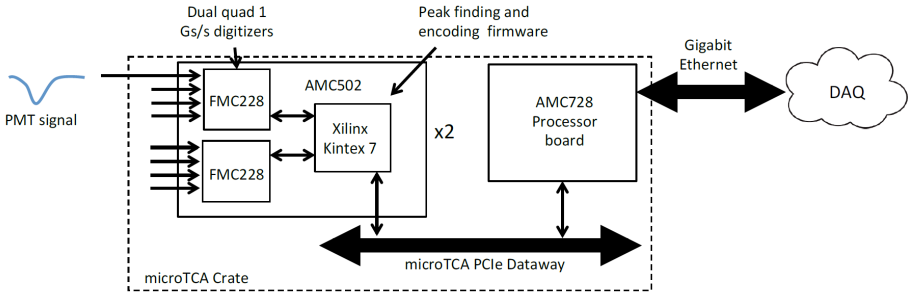

Figure 3.2: The overall setup of the microTCA crate shows all of the components necessary to produce only signals that constitute a peak signal from the PMTs.

3.3 CRV Development

As discussed previously, the purpose of the CRV studies is to account for cosmic-ray muon activity in the Detector and Transport solenoids using the offline analysis. This is done by covering the volume around both solenoids with long extruded scintillation modules to then detect and veto cosmic-ray muons. To accomplish such a task, the extruded scintillation modules must be tested and contain an overall efficiency of 99.99%. This means that it must contain an overall inefficiency of 1×10^{-4} through the filtration of photoelectron (PE) yield requirement which in this case is $>$10 PEs. From this, the di-counters in the modules can be quantified to ensure that they meet the single-layer inefficiency requirement which is 0.4% inefficiency from a four-layer veto to meet the 1×10^{-4} inefficiency requirement.

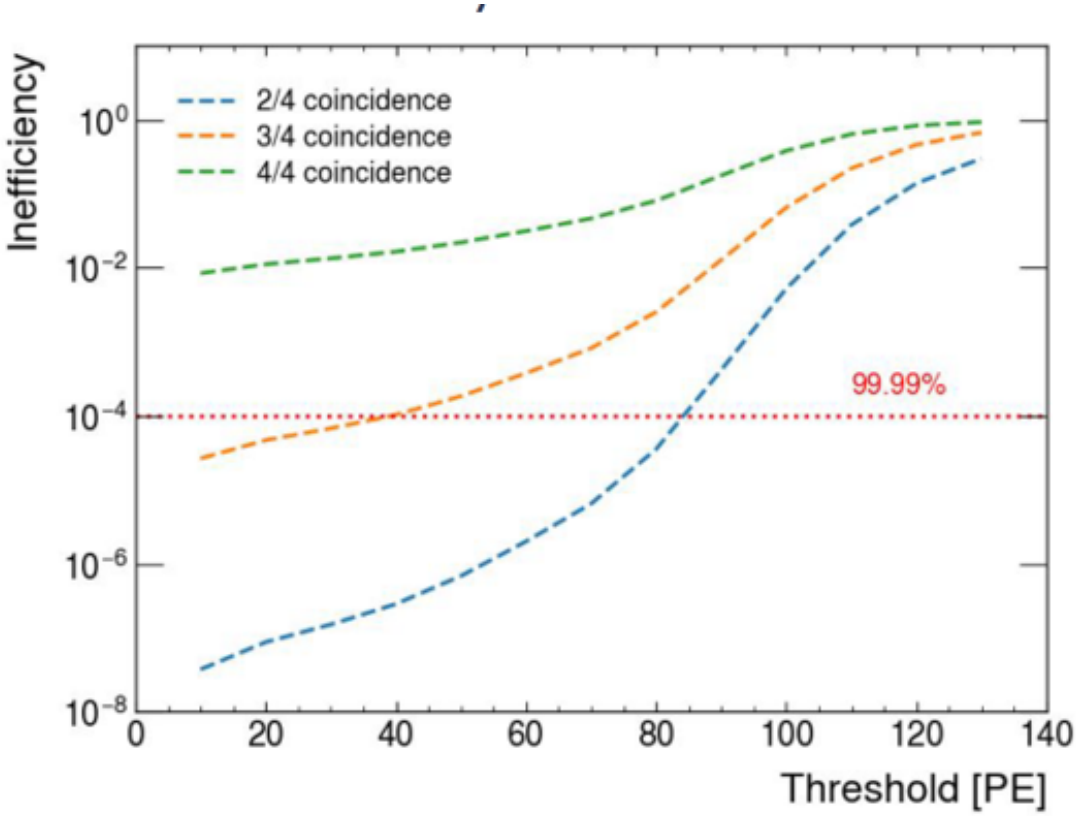

Figure 3.3: Inefficiency plot as a function of photoelectron (PE) threshold showing the 2/4 coincidence data to extrapolate the 3/4 and 4/4 coincidences shown above. It also shows the efficiency/inefficiency requirement.

In the development conducted so far for this project, the inefficiency is analyzed for a triangular counter to determine the effects of the geometry and ”new” rectangular di-counters to quantify the aging effects on the overall inefficiency. Coupled with this, an analysis of the wrapping material of the di-counters themselves is being conducted by seeing how the aging of the material wrapping affects the inefficiency. This is done by wrapping two of the rectangular counters with black insulating tape and the other two with black plastic. Both are used to prevent any light leakage into the counters. The threshold is set to define a hit if $>$10 PEs for both triangular and rectangular counters. The rest of the modules are used as triggers to build the muon tracks where the test counters are situated as seen in Figure 3.4. The single-layer inefficiency of the triangular and the rectangular counters is seen in Figure 3.5.

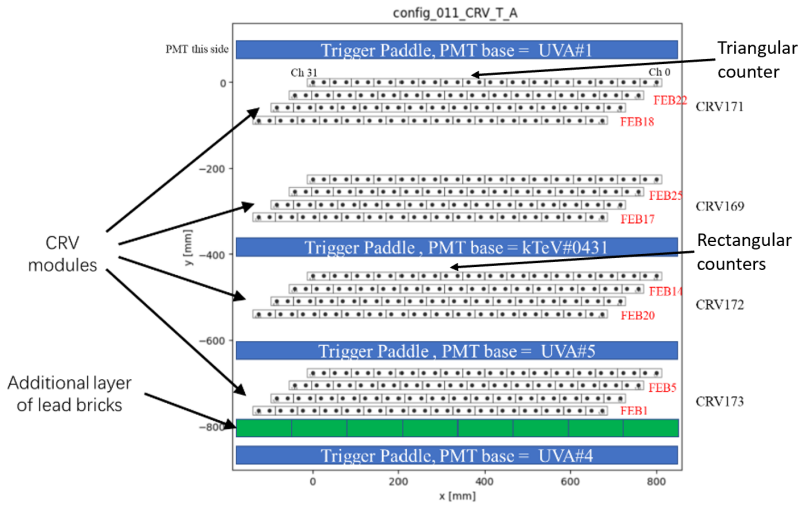

Figure 3.4: The four modules show all the di-counters with the locations of the triangular and rectangular counters. The rest of the panels are used as triggers.

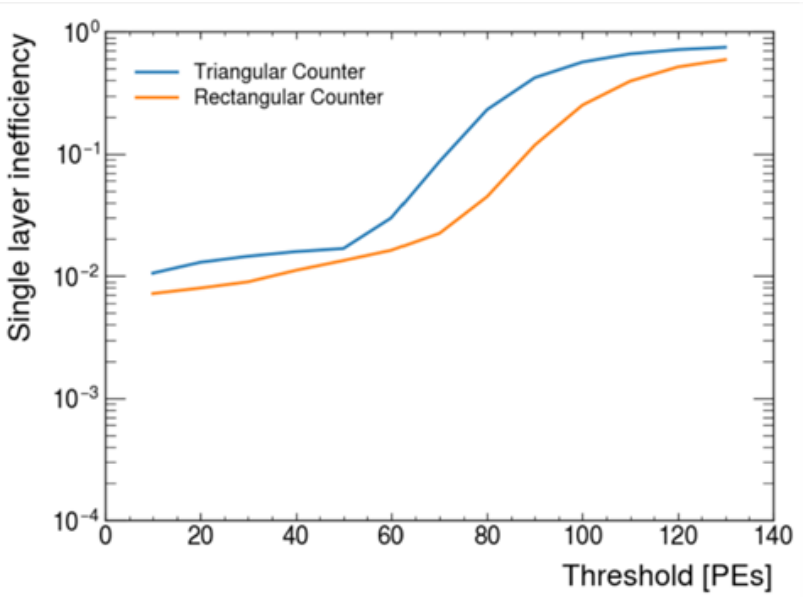

Figure 3.5: Single layer inefficiency of the triangular counter & the four rectangular di-counters using the 4 runs data.

This data was collected in several days per run, with a total of 4 runs. These inefficiencies contain other cosmic activity rather than just muons. Such activity can be showers as seen in Figure 3.6. A potential muon track can be seen in Figure 3.7 as the muon traverses through the CRV modules.

To eliminate such events from the results, further data processing must be conducted to only display linear tracks since cosmic-ray muons have a single linear track as they traverse through the triggers. This linear track feature is implemented in the code that's used to quantify the inefficiency using Python in Jupyter Notebook. After this filtration is complete, the following plots are produced.

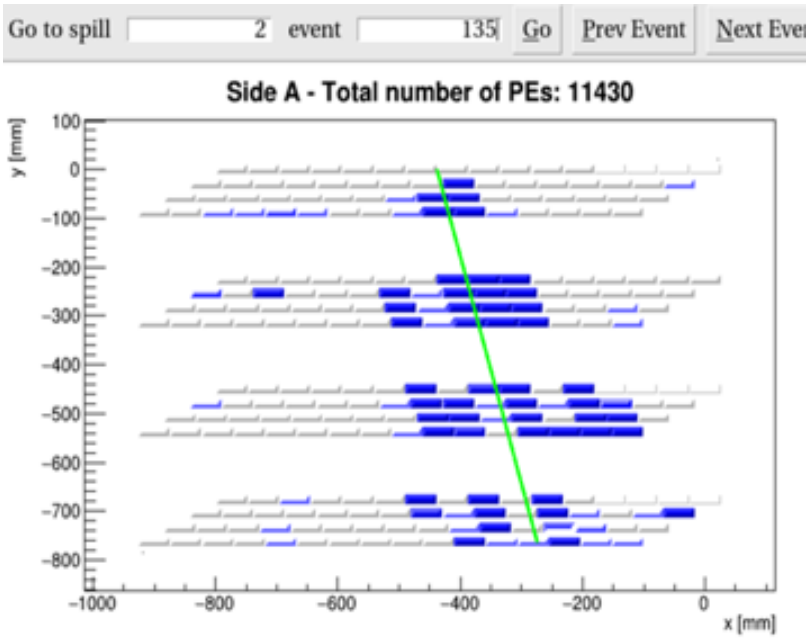

Figure 3.6: A cosmic shower event from the first run.

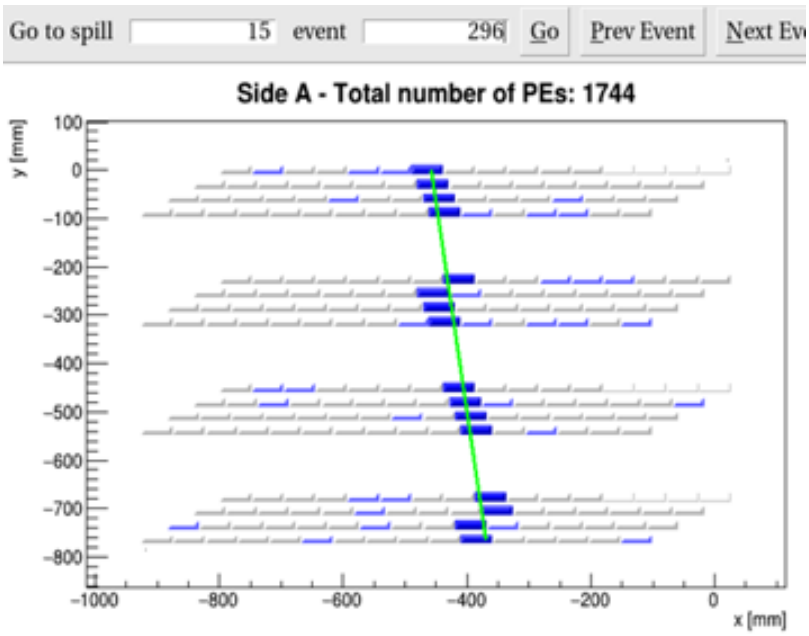

Figure 3.7: Muon track as it passes through the triangular and rectangular counters, producing a track from the trigger counters.

Figure 3.8 shows improvement in the data quality meaning that there's more non-muonic activity being filtered out using the linear track features. It still doesn't improve the data to the 10^{-4} inefficiency requirement on the rectangular di-counters but is an improvement to account for more muon activity.

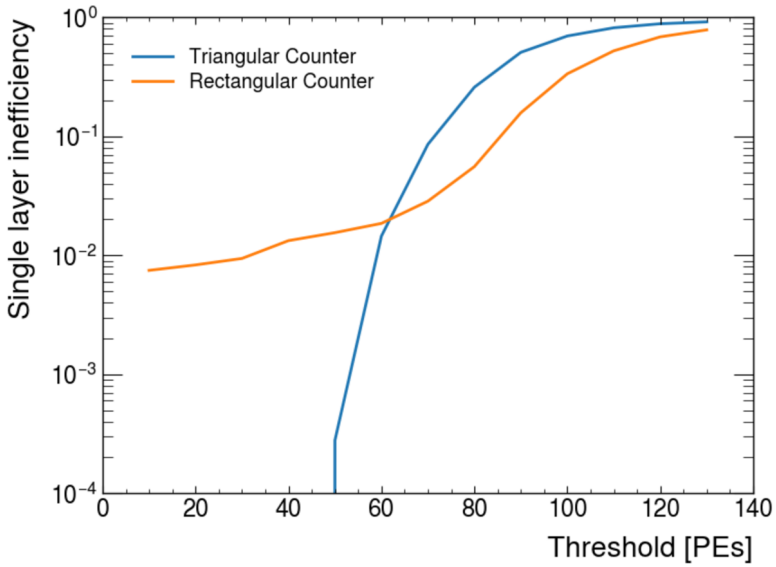

Figure 3.8: A plot showing the triangular counter & the four rectangular di-counters with the implementation of the linear track for further data filtering.

Chapter 4

CONCLUSION

4.1 Conclusion

The work contribution to the Mu2e experiment is seen in each of the projects discussed above. From such contributions, the work done will be able to aid the experiment by using preliminary estimates of a statistical approach on the extinction in the Production target to ensure it's in the order of 10^{-10} using the UEM telescope and the microTCA. The CRV studies will aid the data quality in the Detector Solenoid by accounting for cosmic muons that will mimic the muons of concern through the studies of the most efficient environments for the counters. All of these projects aim to improve the sensitivity of the Mu2e experiment through the verification of temporal pulse distribution by analyzing the out-of-time extinction rates or accounting for background sources that will give misleading results.

4.1.1 Upstream Extinction Monitor Analysis

Once the beam is back on, the extinction rates will be analyzed by setting up the telescope and target. This project will be coupled with the microTCA crate since that's the communications system that'll be used to process the signals and get the processed signal to the data acquisition for further data processing. From this, the extinction levels can be verified.

4.1.2 Supplemental Work

MicroTCA:

The peak-finding algorithm is currently being developed as well as the assembly of the physical crate. As discussed previously, the crate will be used for the extinction rate measurements when the accelerator facilities are up and running. Until then, other work can be done to test both the microTCA crate and the UEM telescope to ensure functionality.

CRV: Due to the time scale of the aging studies on the counters, more work will be conducted at a later time to characterize the aging effects of the counters by analyzing the inefficiencies and comparing them to the results achieved in this first run. Additionally,

more work will be done to understand the wrapping effects of the di-counters to ensure that the best wrapping material is used for the modules in the Mu2e experiment along with how the inefficiency is affected by the shape of the counter. To ensure that there's enough statistical significance in the inefficiencies of the counters, additional work is being done to incorporate a script to allow more runs for data processing without being too demanding on the memory usage of the Jupyter Notebook server.

Appendix A

CODE DETAILS

This chapter presents the code for:

A.1 Upstream Extinction Monitor - Extinction Rate Simulation

Listing A.1: Upstream Extinction Monitor - proton and titanium simulation.

```
#-------------------------------------------#
#          Author: S.BOI & A.BIBIAN         #
#                  kc9qin@gmail.com         #
#                  alexisbibian05@gmail.com #
#          Date: 07/11/2014                 #
#             v2.05/11/2023                 #
#-------------------------------------------#

#-------------------------------------------#
# !!! THE FOLLOWING PARAMETERS ARE DOUBLES !!! #
#-------------------------------------------#

#Number of events to simulate
  param nEvents=1E6
#num crystals, if n=1 you must force k=1 yourself
  param n=1
  param k=1 #($n-1)
  param jmax=($n-1) #this should always be n-1
#radius of first plane
  param r=889.
#arc angle
  param theta=90.
```

```
#distance downstream
  param d=976.83
#length of detector
  param l=1282.7
#side of quartz cube
  param s=18.
#spacing between nearest planes
  param pspace=450.85

param radconv=1/deg

#physics list
physics QGSP_BERT

#Define a random event
randomseed Time



#--------#
# FILTER  #
#--------#
#sets a lower limit on the kinetic energy needed to produce
    Cherenkov radiation & filters neutral particles
trackcuts kineticEnergyCut=0.1738 keep=pi+,pi-,mu+,e-,
   proton,mu-,gamma,e+

#pulled this material from internet: density was 2.66, SiO2
    so 1:2 ratio of Si-O
material QUARTZ density=2.66 Si,0.335 O,0.665

#KE is in MeV
param M=938.272 KE=8000.0
param P=sqrt(($KE+$M)*($KE+$M)-($M*$M))

# the beam is nominally headed in the +Z direction
beam gaussian particle=proton nEvents=$nEvents beamZ=-1.0 \
        sigmaX=0.25 sigmaY=0.25 sigmaXp=0.0 sigmaYp=0.0 \
        meanMomentum=$P sigmaP=0.0 meanT=0.0 sigmaT=0.0
```

```
#------------------#
# BEAMLIME GEOMETRY #
#------------------#
cylinder Target radius=38.1 length=0.008 material=Ti color
   =0.5,0.5,0.5
tube SteelTube innerRadius=38.1 radius=39.6 length=100
   initialPhi=0 finalPhi=360 material=STAINLESS-STEEL color
   =0.85,0.85,0.85
cylinder DeathKillDestroy radius=39.6 length=100. color
   =1,0,0 kill=1
box subVol height=$s width=$s length=200.
boolean op=subtraction Killer DeathKillDestroy subVol x=0 y
   =0 z=-50. rotation=Y-(atan($r/$d)*$radconv)
virtualdetector crystal require= height=$s width=$s length=
   $s color=1,1,1,0.2 material=QUARTZ format=BLTrackFile

place Target z=0 rename=target
place Killer z=1. front=1 kill=1
place DeathKillDestroy z=-52



#-------------#
# PMT GEOMETRY #
#-------------#
material DHOUSING density=0.594 Al,1

cylinder dividerhousing radius=21 length=82 material=
   DHOUSING \
    color=0.45,0.4,0

tubs blackshielding innerRadius=18.2 outerRadius=21 length
   =118 material=Zn \
    color=0.05,0.05,0.05

tubs rolledshield innerRadius=15.5 outerRadius=16.7 length
   =117 material=Ni \
    color=0.85,0.85,0.85
```

```
tubs glassportion innerRadius=13 outerRadius=14.5 length
   =88. material=Pyrex_Glass \
    color=1,1,1,0.2

cylinder glasswindow radius=14.5 length=3. material=
   Pyrex_Glass color=1,1,1,0.2

group pmt radius=21
  place dividerhousing x=0. y=0. z=118 front=1
  place blackshielding x=0. y=0. z=0. front=1
  place rolledshield x=0. y=0. z=0.5 front=1
  place glassportion x=0. y=0. z=14.5 front=1
  place glasswindow x=0. y=0. z=0. front=1
  place glasswindow x=0. y=0. z=102.5 front=1
endgroup


#-------------------#
# TELESCOPE GEOMETRY #
#-------------------#
do j 0 $jmax
  place crystal z=$d x=$r*cos(($j*($theta/$k))/$radconv) y=
   $r*sin(($j*($theta/$k))/$radconv) rotation=Y((atan($r/$d)
   )*$radconv),Z(($j*($theta/$k))) rename=det$j@0
  place pmt front=1   z=$d-(($s/2)*sin(atan($r/$d))) x=$r*
   cos(($j*($theta/$k))/$radconv)+(($s/2)*cos(($j*($theta/$k
   ))/$radconv)) y=$r*sin(($j*($theta/$k))/$radconv)+(($s/2)
   *sin(($j*($theta/$k))/$radconv)) rotation=Y(90+(atan($r/
   $d)*$radconv)),Z(($j*($theta/$k)))

  place crystal z=(sqrt(pow($r,2)+pow($d,2))+$pspace)*cos(
   atan($r/$d)) x=(sqrt(pow($r,2)+pow($d,2))+$pspace)*sin(
   atan($r/$d))*cos(($j*($theta/$k))/$radconv) y=(sqrt(pow(
   $r,2)+pow($d,2))+$pspace)*sin(atan($r/$d))*sin(($j*(
   $theta/$k))/$radconv) rotation=Y((atan($r/$d))*$radconv),
   Z(($j*($theta/$k))) rename=det$j@1
  place pmt front=1   z=((sqrt(pow($r,2)+pow($d,2))+$pspace
   )*cos(atan($r/$d)))-(($s/2)*sin(atan($r/$d))) x=((sqrt(
```

```
    pow($r,2)+pow($d,2))+$pspace)*sin(atan($r/$d))*cos(($j*(
    $theta/$k))/$radconv))+(($s/2)*cos(($j*($theta/$k))/
    $radconv)) y=((sqrt(pow($r,2)+pow($d,2))+$pspace)*sin(
    atan($r/$d))*sin(($j*($theta/$k))/$radconv))+(($s/2)*sin
    (($j*($theta/$k))/$radconv)) rotation=Y(90+(atan($r/$d)*
    $radconv)),Z(($j*($theta/$k)))


   place crystal z=(sqrt(pow($r,2)+pow($d,2))+($l-$pspace))*
    cos(atan($r/$d)) x=(sqrt(pow($r,2)+pow($d,2))+($l-$pspace
    ))*sin(atan($r/$d))*cos(($j*($theta/$k))/$radconv) y=(
    sqrt(pow($r,2)+pow($d,2))+($l-$pspace))*sin(atan($r/$d))*
    sin(($j*($theta/$k))/$radconv) rotation=Y((atan($r/$d))*
    $radconv),Z(($j*($theta/$k))) rename=det$j@2
   place pmt front=1   z=((sqrt(pow($r,2)+pow($d,2))+($l-
    $pspace))*cos(atan($r/$d)))-(($s/2)*sin(atan($r/$d))) x
    =((sqrt(pow($r,2)+pow($d,2))+($l-$pspace))*sin(atan($r/$d
    ))*cos(($j*($theta/$k))/$radconv))+(($s/2)*cos(($j*(
    $theta/$k))/$radconv)) y=((sqrt(pow($r,2)+pow($d,2))+($l-
    $pspace))*sin(atan($r/$d))*sin(($j*($theta/$k))/$radconv)
    )+(($s/2)*sin(($j*($theta/$k))/$radconv)) rotation=Y(90+(
    atan($r/$d)*$radconv)),Z(($j*($theta/$k)))

   #place crystal z=(sqrt(pow($r,2)+pow($d,2))+$l)*cos(atan(
    $r/$d)) x=(sqrt(pow($r,2)+pow($d,2))+$l)*sin(atan($r/$d))
    *cos(($j*($theta/$k))/$radconv) y=(sqrt(pow($r,2)+pow($d
    ,2))+$l)*sin(atan($r/$d))*sin(($j*($theta/$k))/$radconv)
    rotation=Y((atan($r/$d))*$radconv),Z(($j*($theta/$k)))
    rename=det$j@3
   #place pmt front=1   z=((sqrt(pow($r,2)+pow($d,2))+$l)*cos
    (atan($r/$d)))-(($s/2)*sin(atan($r/$d))) x=((sqrt(pow($r
    ,2)+pow($d,2))+$l)*sin(atan($r/$d))*cos(($j*($theta/$k))/
    $radconv))+(($s/2)*cos(($j*($theta/$k))/$radconv)) y=((
    sqrt(pow($r,2)+pow($d,2))+$l)*sin(atan($r/$d))*sin(($j*(
    $theta/$k))/$radconv))+(($s/2)*sin(($j*($theta/$k))/
    $radconv)) rotation=Y(90+(atan($r/$d)*$radconv)),Z(($j*(
    $theta/$k)))
enddo
```

Bibliography

[1] R. M. Carey. “Mu2e Proposal”. In: (). Mu2e-doc-388.

[2] David Measday. “The Physics of Muon Capture”. In: Physics Reports 354, 243-409 (2001).

[3] T. J. Roberts, K. Beard, et al. “G4BEAMLINE PARTICLE TRACKING IN MATTER-DOMINATED BEAM LINES”. In: (2008).

[4] E. Prebys et al. “STATISTICAL MEASUREMENT OF LONGITUDINAL BEAM HALO IN THE FERMILAB RECYCLER”. In: *JACoW Publishing* (2019). DOI: https://doi.org/10.18429/JACoW-IPAC2019-WEPGW106.

[5] S. Werkema. “Mu2e Proton Beam Longitudinal Structure”. In: Mu2e-doc-2771 (2019).

[6] C. Polly and E. Prebys. “Extinction Monitor Requirement”. In: (2014). Mu2e-doc-894. URL: https://indico.fnal.gov/event/10361/attachments/1463/1694/extinctReq-v18.pdf.

[7] T. Roberts. “G4beamline User’s Guide”. In: (2017). URL: http://g4beamline.muonsinc.com.

[8] E. Craig Dukes. “Mu2e Cosmic Ray Veto Requirements”. In: (2016). Mu2e-doc-944.

[9] R. Ehrlich, E. Craig Dukes, and Y. Oksuzian M. Frank. “Cosmic Ray Induced Backgrounds”. In: (2018). Mu2e-doc-3059.

[10] L. Bartoszek et al. “Mu2e Technical Design Report”. In: (2015). URL: https://arxiv.org/abs/1501.05241v2.

ACKNOWLEDGEMENTS

The work presented in this note would not be possible without the following acknowledgments so I would like to give a big thank you to all of them. Specially, Steven Boi and Ryan Hooper since they were my supervisor and advisor, respectively, thank you! Additionally, I would also like to thank the following people for aiding my SULI experience: Eric Prebys, Yuri Oksuzian, & SULI staff (Fermilab, Batavia, Illinois).

Last, but not least, there are no words to show my appreciation for my family members and friends since they were my biggest emotional supporters throughout these past few months. Especially my mother, so I thank each and every one of them.

This manuscript has been authored by Fermi Research Alliance, LLC under Contract No. DE-AC02-07CH11359 with the U.S. Department of Energy, Office of Science, Office of High Energy Physics.

This work was supported in part by the U.S. Department of Energy, Office of Science, Office of Workforce Development for Teachers and Scientists (WDTS) under the Science Undergraduate Laboratory Internships Program (SULI).